Journal of
Plankton Research

academic.oup.com/plankt

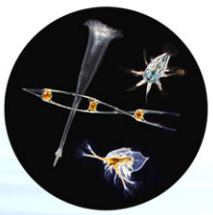

J. Plankton Res. (2018) 00(00): 1–14. doi:10.1093/plankt/fby025

Vertical structure of plankton communities in areas of European eel larvae distribution in the Sargasso Sea

PETER MUNK[1]*, TORKEL GISSEL. NIELSEN[1], CORNELIA JASPERS[1,2], DANIEL J. AYALA[1], KAM W. TANG[3], FABIEN LOMBARD[4] AND LASSE RIEMANN[5]

[1]NATIONAL INSTITUTE OF AQUATIC RESOURCES, SECTION FOR OCEANS AND ARCTIC, TECHNICAL UNIVERSITY OF DENMARK, LYNGBY 2800, DENMARK, [2]DEPARTMENT OF EVOLUTIONARY ECOLOGY OF MARINE FISHES, HELMHOLTZ CENTRE FOR OCEAN SCIENCE, GEOMAR, KIEL 24105, GERMANY, [3]DEPARTMENT OF BIOSCIENCES, SWANSEA UNIVERSITY, SWANSEA SA2 8PP, UK, [4]SORBONNE UNIVERSITÉ, CNRS-INSU, LABORATOIRE D'OCÉANOGRAPHIE DE VILLEFRANCHE, LOV UMR 7093, VILLEFRANCHE-SUR-MER F-06230, FRANCE AND [5]MARINE BIOLOGY SECTION, DEPARTMENT OF BIOLOGY, UNIVERSITY OF COPENHAGEN, HELSINGØR 3000, DENMARK

*CORRESPONDING AUTHOR: pm@aqua.dtu.dk

Received January 16, 2018; editorial decision May 31, 2018; accepted June 4, 2018

Corresponding editor: Xabier Irigoien

The European and American eels spawn in the subtropical convergence zone (STCZ) in the Sargasso Sea, a dynamic and relatively productive area that is strongly influenced by front and eddy formations and subducted high-saline water masses. To understand how the physical and biological environments may affect the early life history of eels, we conducted a detailed bio-physical investigation of the water column at a site of high eel larvae abundance. Diel measurements and sampling in the upper 300 m revealed strong variations in hydrographic conditions and mean depths of different taxonomic groups; however, characteristics patterns of distribution were apparent. Most species showed diel vertical migrations, ascending about 20–30 m at night, whereas examples of night–time downward migration were also seen. European eel larvae were among the species showing more extensive diel vertical migration: their population mean depth changed from 160 m at day to 100 m at night where abundance peaked at 45 m depth. Distribution and migration of eel larvae corresponded to patterns observed for small hydrozoans, supporting a proposed predator-prey linkage. The study demonstrates the diverse and vertically strongly structured plankton community of STCZ where larvae of eel and other fish find a wide range of potential niches.

KEYWORDS: vertical migration; plankton communities; leptocephali larvae; freshwater eels; subtropical convergence zone

available online at academic.oup.com/plankt

INTRODUCTION

The subtropical convergence zone (STCZ) in the Sargasso Sea is known to be a hotspot for spawning of Atlantic eels (Schmidt, 1923; Miller *et al.*, 2014). Due to a sharp decline in recruitment to the eel populations in the recent decades, there is a strong demand for further understanding of the temporal and spatial variabilities in the bio-physical characteristics of the zone and how they may influence recruitment success. In the STCZ, warm tropical water meets colder North Atlantic water masses and the zone is bordered by hydrographic fronts of changing intensity and location (Eriksen *et al.*, 1991, Ullman *et al.*, 2007). Furthermore, the STCZ is characterized by significant eddy formation (Halliwell *et al.*, 1991) leading to intensive mixing in the upper 200–300 m (Munk *et al.*, 2010; Richardson and Bendtsen, 2017). While the deep current (the North Equatorial Current) is directed towards the west, the upper layers in the zone might in some areas flow north-east along the zonal density fronts, forming an eastward subtropical counter current (Cushman-Roisin, 1984). A thermocline is present at 100–150 m and an intrusion of more saline water originating from the equatorial areas is often seen at 80–150 m (Williams, 2001). The pronounced variability in the horizontal and vertical hydrography is likely to affect the structuring of plankton communities in the area with further influence on the early development of the anguillid eels (*Anguilla anguilla* and *A. rostrata*).

Studies of the plankton communities in the Sargasso Sea often target areas north of the STCZ, in particular the site of the Bermuda Atlantic Time-series Study (BATS) (reviewed by Steinberg *et al.*, 2001). Conditions in these colder North Atlantic waters are, however, not comparable to the STCZ, where the different hydrography would favor different plankton communities (Longhurst, 1985). Studies specifically targeting central areas of the STCZ have found an enhanced abundance of primary producers (Riemann *et al.*, 2011) and elevated productivity (Richardson and Bendtsen, 2017). Although the Sargasso Sea is generally considered as oligotrophic with a predominance of picoplankton (Gasol *et al.*, 1997), the biomass of large protists, such as athecate dinoflagellates and ciliates, has been found to equal or exceed that of picoplankton within the STCZ (Riemann *et al.*, 2011), probably leading to a locally enhanced mesozooplankton production. An enhancement in a number of metazoan groups, e.g. copepods and appendicularians, has been observed in central areas on STCZ (Munk *et al.*, 2010; Andersen *et al.*, 2011). Furthermore, fish larvae including those of European and American eels have been found in relatively high abundances within STCZ, with declining abundances when passing the fronts towards waters outside the STCZ (Ayala *et al.*, 2016).

In addition to horizontal variability in plankton community composition and abundances in the STCZ, variability is also apparent along the vertical axis, where most plankton taxa are concentrated in specific depth strata (Andersen *et al.* 2011; Riemann *et al.*, 2011). The published information on vertical distribution of fish larvae in the STCZ is restricted to distributional patterns of leptocephali larvae. In the western Sargasso, Miller (2015) found the majority of leptocephali larvae in the upper 100 m at night, with several species (including *Anguilla rostrata*) concentrated within the 50–60 m depth. Likewise, Castonguay and McCleave (1987) observed that at night–time, *Anguilla* spp. larvae were concentrated within 50–70 m. *Anguilla* spp. larvae have been observed to perform marked diel vertical migrations (DVMs), descending to 100–200 m depth during the day (Schoth and Tesch, 1982). However, only a few eel larvae have been found below a depth of 200 m (Schmidt, 1923; Castonguay and McCleave, 1987).

The early life of fishes in the STCZ, including the *Anguilla* spp., is governed by the specific physical, chemical and biological characteristics of available habitats in the water column. In order to gain further understanding of opportunities and constraints to the life of *Anguilla* spp. larvae, we here investigate in detail the water column properties and the structuring of the plankton community of the STCZ, looking for commonalities and differences between community members. We included several trophic levels, ranging from algae and microplankton, to mesozooplankton and macroplankton, and finally onto the fish larvae. The study was carried out during a larger field investigation at a site of relative high abundances of *Anguilla* spp, and we hypothesized that the eel larvae occupy a specific niche in the community, defined by their vertical position, their diel migration pattern and their linkages to specific hydrographical and biological characteristics.

MATERIALS AND METHODS

Intensive sampling was conducted at 25°38′ N, 62°48′W from 31 March 13:46 UTM to 1 April 14:20 UTM, 2014 on board of the R/V Dana (local time was UTM—4 h). The site was part of a survey transect across the STCZ, extending along 62°45′W from 24°40′N to 29°50′N (Fig. 1), and was chosen for the relatively high *A. anguilla* abundances observed during the standard transect sampling.

Profiles of temperature, salinity, fluorescence, oxygen and irradiance were measured from surface to 400 m

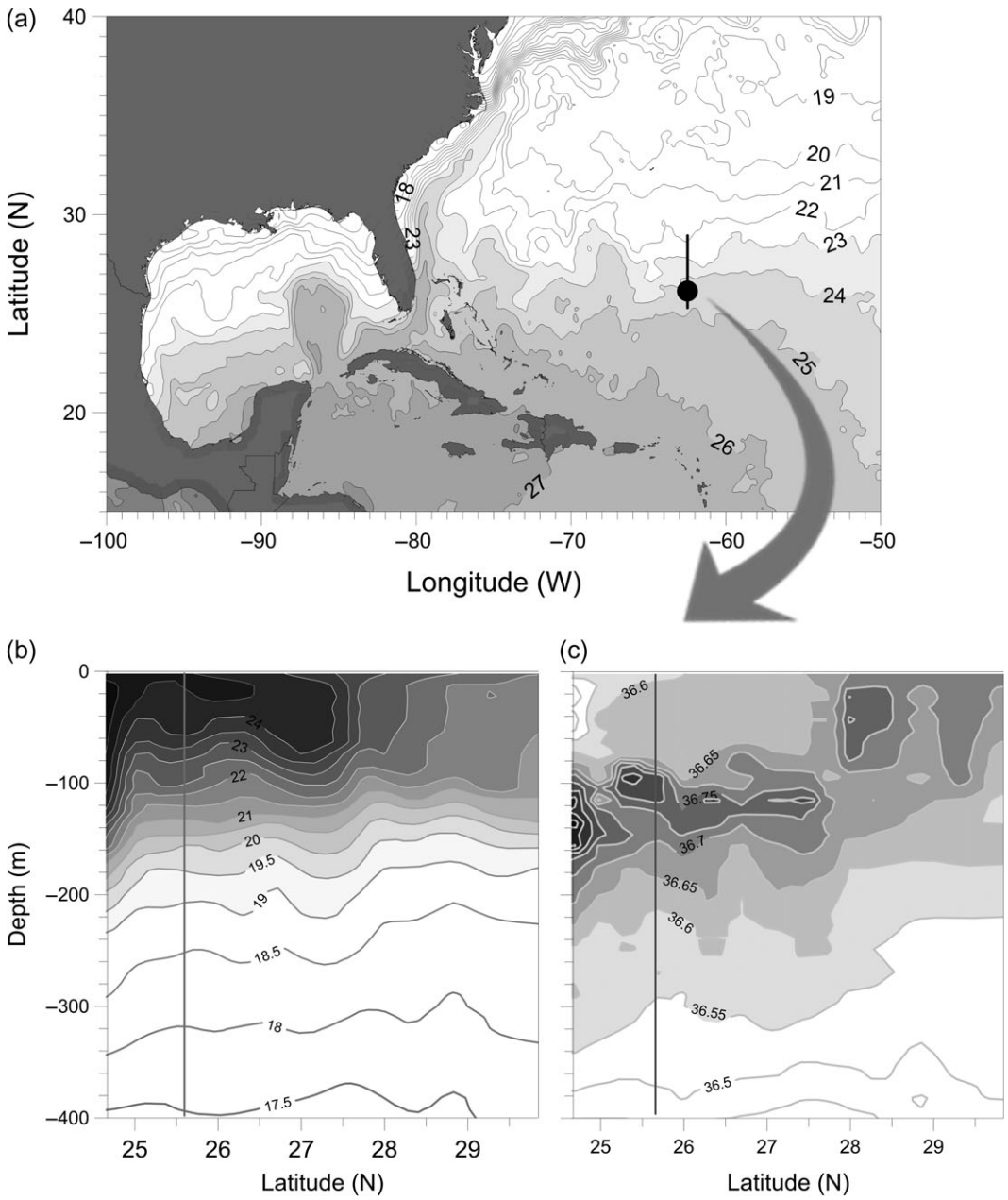

Fig. 1. Area of sampling. (**a**) Transect at 62°45′W (line) and sampling position (dot) in the southern Sargasso Sea for this study; contour lines indicate SST from satellite observations. Hydrographical sections along the transect for (**b**) temperature (°C) and (**c**) salinity; vertical lines indicate sampling position for the vertical study.

depth by a Seabird SBE11 (9+) CTD, with mounted Biospherical QSP-2300L PAR Sensor, SBE 43 Dissolved Oxygen Sensor, and Turner Cyclops-7 Fluorometer. Silicate, nitrite, nitrate and chlorophyll *a* were measured in subsamples from ten-liter Niskin bottle samples taken at 10, 30, 60, 85, 130, 155, 255 and 400 m depths.

An Underwater Video Profiler (UVP5, serial number Sn003, pixel size ca. 0.147; Picheral *et al.*, 2010) was deployed alongside the CTD to 400 m. The device emitted flashes of red LED light that illuminated 0.93 L of the water. Images of all particles within the illuminated area were recorded and analyzed for abundances in defined size ranges. Objects larger than 30 pixels were further analyzed by a taxonomist. Here we only report observations of particles in three size ranges: small (0.05–0.53 mm), medium (0.53–1.06 mm) and large (1.06–4.0 mm).

Microzooplankton (ciliates and heterotrophic dinoflagellates) were analyzed using water subsamples from 10-L

Niskin bottle samples taken at 10, 30, 60, 85, 130, 155, 255 and 400 m depths. These were immediately fixed with acid Lugol's solution (2% final concentration) and stored in the dark at 5°C until analysis. For the analysis, protozoans were allowed to settle for 24 h in 50-mL sedimentation chambers, and were then enumerated and sized under an inverted microscope (Utermöhl, 1958). Cells were identified to the lowest possible taxonomic level and grouped by equivalent spherical diameter intervals of 10 µm. Cell volumes were estimated from appropriate geometric formulae and converted to carbon content. All athecate dinoflagellates of unknown trophy were considered heterotrophic (Andersen *et al.*, 2011).

Zooplankton samples were collected using a multiple opening-and-closing net (Multinet Midi, HydroBios®, 0.25 m^2 mouth opening) in seven discrete depth intervals (0–25, 25–65, 65–100, 100–135, 135–180, 180–230 and 230–280 m). Zooplankton in the micro- and mesozooplankton size range were sampled by hauling vertically a 45 µm mesh Multinet from 280 m to the surface, while rare and larger sized zooplankton were sampled during an oblique haul with a 335 µm mesh Multinet lowered to 280 m and retrieved to the surface at a speed of 2 knots. For the 45 µm Multinet sampling, the water volume filtered per net ranged from 5 to 13 m^3. Samples were preserved in 4% Borax buffered formalin, and after the cruise the zooplankton were identified, enumerated and measured for total length, and cephalothorax length for copepods.

Fish larvae and gelatinous macrozooplankton were sampled using a conical ring net (MIK, 3.5 m diameter opening, 25 m total length, 560 µm body mesh size with 330 µm mesh for the hindmost 1 m and the cod end). The net was lowered to a given depth, measured by a mounted depth sensor (Scanmar®), using a fast wire pay-out, and towed at 2 knots for 40 min. Tow depth varied by ±3 m during tows. Afterward, the net was retrieved at a high speed. Filtrating during the pay-out and retrieval phase was assumed to be ineffective at such high speed. The effective volume filtered was estimated from the tow path at depth apparent from the recorded profile of the depth sensor. Six discrete depths were sampled (45, 85, 120, 155, 205 and 255 m) during day (12:00–18:00 local time) and night (00:00–06:00 local time). Upon retrieval, the net was washed down and the cod end content was transferred to 20-L transparent buckets (Cambro®). The buckets were kept on ice during processing, and the content was examined for fish larvae and gelatinous macrozooplankton (excluding siphonophores) within 45 min.

Gelatinous zooplankton were identified and measured alive using a dark field light table in transparent plexiglass trays. After the screening, 10% of the MIK sample was preserved in 4% buffered formalin solution for later estimation of siphonophore abundance. Siphonophore abundance was difficult to estimate due to their colonial structure and tendency to disintegrate. However, the sampled siphonophore community consisted primarily of Calycophorans, hence we used only the anterior nectophore of the polygastric stage for species identification and enumeration (Bouillon *et al.*, 2004). Very few bracts of the sexual eudoxid stage were encountered.

Observed fish larvae were directly preserved in 96% ethanol, the leptocephali after being length measured in a stereomicroscope-video setup. The remainder of the sample was preserved in ethanol for later sorting, identification and measurement of fish larvae that were not observed during the initial screening. All length measurements were made to larval standard length. Fish larvae visually identified as *Anguilla* spp. were later verified as either *A. anguilla* or *A. rostrata* using molecular markers (Jacobsen *et al.*, 2017). Identification of other larval fish species was based on type specimens from an earlier study in the same area (Ayala *et al.*, 2016).

Information on the distribution and diel migration of acoustically reflecting organisms were obtained from a ship-mounted Simrad® EK60 38 kHz echosounder, which was run continuously during the vertical study. Signals were analyzed by Echoview® software, and data on volume backscatter at depth were interpolated using the Surfer® program.

Data analyses

Distributional mean depths (MD) of plankton size intervals, genera or species were calculated as:

$$\mathrm{MD} = \sum_{k=0}^{n} D_k * W_k * C_k / \sum_{k=0}^{n} W_k * C_k$$

where D_k is mean depth of stratum k (m), W_k is width of stratum k (m) and C_k is the estimated density of organisms in stratum k (no m^{-3}).

For analysis of commonalities and differences in vertical distributions of plankton taxa, we calculated a similarity matrix combining a double hierarchical classification and an ordered heatmap representation. The method considered Euclidean distances with a "complete link" classification. To compare both abundant and non-abundant taxa, we used proportions in strata and solely strata in 45 m and below, since some taxa were not sampled in the uppermost stratum. In a schematic representation, the taxa were organized and grouped according to similarity in their relative abundances at depth.

RESULTS

Hydrography

The sampling site was positioned ca. 100 km north of the southern front of the STCZ. This front was characterized by declining isotherms at the southernmost part of the transect (Fig. 1b). Water temperature was ca. 24–24.5°C in a mixed water layer extending to about 80 m depth. Below this layer a wide thermocline was apparent, with a decline in temperature to 19°C at 150 m (Fig. 2a). Salinity was 36.6 in the mixing zone, and deeper, between 80 and 160 m depth, an intrusion of more saline water (~36.8) was apparent (Figs 1c and 2a). The intrusion at this sampling site had a double structure, a pattern also observed at other stations during the cruise. Further below the salinity declined, reaching 36.42 at 400 m and continuing the decline until at least the depth of 1000 m (nearby CTD cast, data not shown).

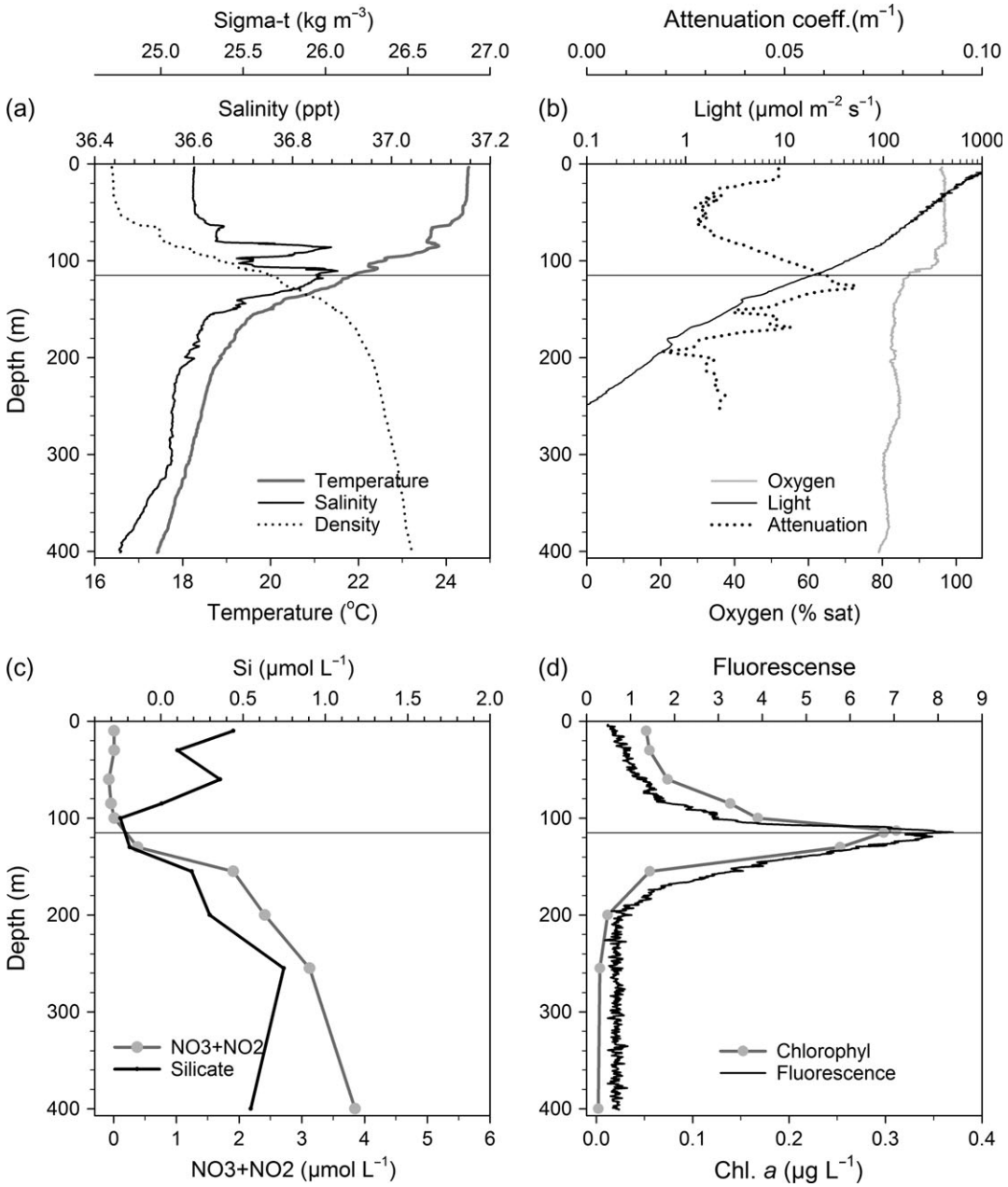

Fig. 2. Depth profiles at the vertical study site: (**a**) Temperature, salinity and water density; (**b**) oxygen, light radiance and light attenuation coefficient; (**c**) NO3+NO2 and silicate; and (**d**) fluorescence and chlorophyll *a*. Measurements in (a) and (b) and fluorescence are from CTD cast; measurements in (c) and chlorophyll *a* are from water bottle sampling.

Light levels measured at 14:30 UTM declined from 1000 μmol m^{-2} s^{-1} at 10 m to 40 μmol m^{-2} s^{-1} at 100 m and 1.5 μmol m^{-2} s^{-1} at 160 m (Fig. 2b), and were below the detection limit at depths below 250 m. The attenuation coefficient varied through the water column, showing peaks in the immediate surface layer and the in association with the deep chlorophyll *a* layer (Fig. 2b). Dissolved oxygen level was near 100% saturation in the upper 100 m but showed an abrupt drop to about 80% across the upper thermocline, and stayed at this level further below (Fig. 2b). Nitrate+nitrite levels were low in the upper 110 m (<0.25 μmol L^{-1}), increased to 2 μmol L^{-1} at 130 m and increased further at greater depths (Fig. 2c). Silicate levels were in the order of 1–2 μmol L^{-1}, but were markedly lower between 60 and 130 m (Fig. 2c).

Microplankton and snow particles

The CTD fluorometer and extracted chlorophyll measurements showed similar vertical profiles of algal concentrations (Fig. 2d). In the mixing zone at 0–80 m depth, the chlorophyll *a* concentration was low (~0.08 μg L^{-1}), but it increased further below and peaked in a deep chlorophyll maximum (DCM) of 0.32 μg L^{-1} at about 120 m depth. Below the DCM, the chlorophyll *a* concentration declined markedly to near zero at 200 m depth.

Particles detected by the Underwater Vision Profiler (UVP) were categorized into three groups based on their equivalent spherical diameter (Fig. 3a). All three groups were found in high abundances near the surface, but they differed in their vertical distributions throughout the water column. Small particles showed a subsurface minimum of ~15 particles L^{-1} in the depth range 20–60 m, increasing to 25 particles L^{-1} at 160–200 m. In contrast, abundances of both medium and large particles steadily decreased with depth, reaching near zero particles below 250 m. Two characteristic components of the medium and large sized particles were identified as *Trichodesmium* colonies and radiolarians (Rhizaria) (Fig. 3b). Both of these showed highest abundances above 60 m with another enhancement in abundance at 120–140 m (Rhizaria) or 140–200 m (*Trichodesmium*). Concentrations of ciliates and heterotrophic dinoflagellates based on bottle sampling showed both their highest levels above 150 m, but their peaks of abundance in the water column differed (Fig. 3c). The dinoflagellates peaked close to the DCM, while abundances of ciliates were high in the mixed layer and showed a secondary peak below the DCM.

Mesozooplankton

The vertical profile of total mesozooplankton from the 45-μm Multinet sampling showed a characteristic peak at the surface, another at the 65–100 m depth interval, and very low abundances below 180 m (Fig. 4a, Supplementary Table S1). Diel changes in the combined vertical distribution of the community in the investigated upper 250 m were marginal, with a weak tendency of night–time descent. There was, however, great variability in distribution patterns among the different taxonomic groups (Supplementary Fig. S1, Table S1). For example, *Oncaea* sp. showed no surface peak, (Fig. 4g and h), while *Oithona* sp. copepods (Fig. 4c) were distributed relatively deep with a peak around 150 m. Hydrozoans as *Amphicaryon acaule* and *Bougainvillia niobe* were distributed deep at day and shallower at night (Fig. 4k and l). Additional differences were apparent within taxa for the naupliar and copepodite stages of copepods; e.g.

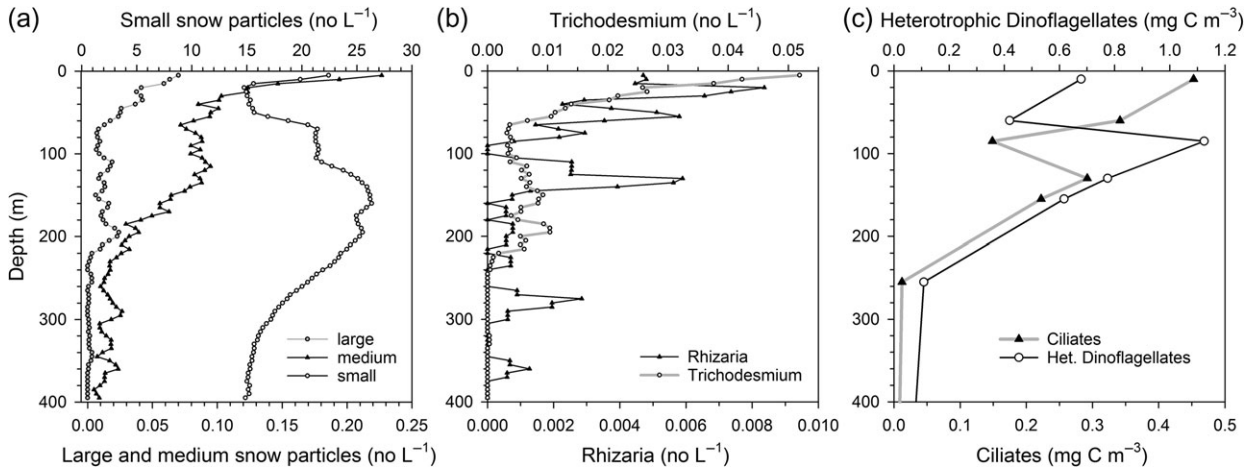

Fig. 3. Abundances of (**a**) Marine snow (0.05–0.53, 0.53–1.06, 1.06–4.0 mm); (**b**) *Trichodesmium* and Rhizaria; and (**c**) ciliates and heterotrophic dinoflagellates. Measurements in (a) and (b) are from profiling by video recorder; measurements in (c) are from water bottle sampling.

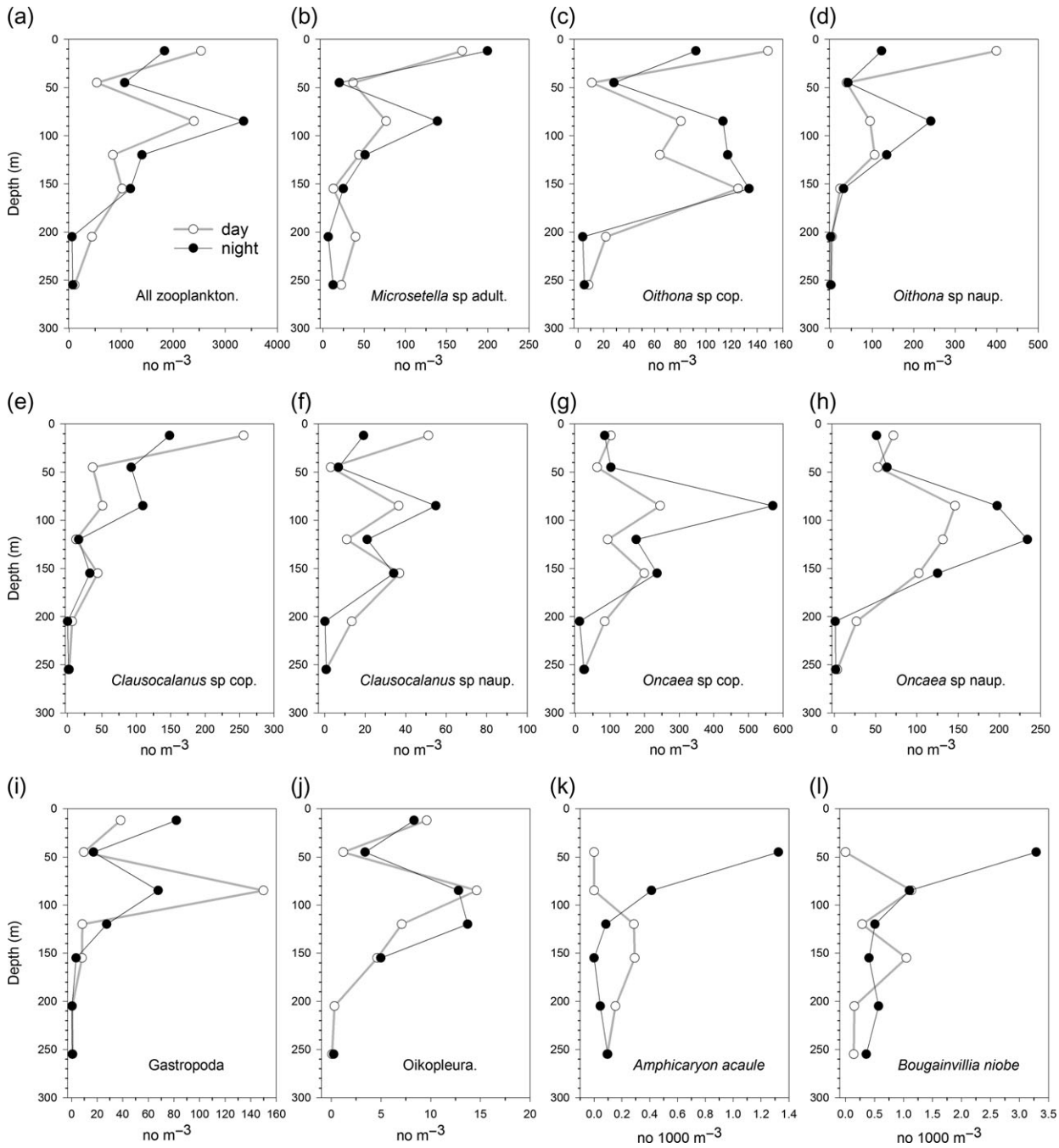

Fig. 4. Day (open symbol) and night (closed symbol) vertical distributions of selected plankton taxa and stages. (**a**)–(**j**) Mesozooplankton profiles based on 45 μm vertical Multinet hauls in strata, average abundances in stratum (no. m^{-3}). (**k** and **l**) Macrozooplankton profiles based on horizontal 550 μm MIK net hauls at depth (no. 1000 m^{-3}).

Clausocalanus spp. nauplii tended to be deeper (Fig. 4e and f) while *Oithona* sp. nauplii tended to be shallower (Fig. 4c and d) compared to the respective copepodite stages.

The vertical distributions and migration patterns of mesozooplankton were related to size of organisms (Fig. 5a). There was a general decline in MD, both for the copepods and for the group of other mesozooplankton. For the copepods the MD was about 70 m for length <500 μm, and at these sizes (including the nauplii stages) the distances of DVM were minor (<10 m). In the copepod length range of 500–1000 μm, the MD declined from the 70 to 90 m depth, with a DVM of 20–30 m (ascent at night). The largest size

group for which the MD could be calculated (1300 µm) was found at depth 110–140 m and showed a night–time decent; this group was dominated by *Haploptilus* spp., which had an uncommon DVM behavior (Fig. 5b and c). In the group of non-copepod zooplankton, there was a more pronounced influence from size, and MD changed from 20–60 m to 90–130 m across the length range 100–900 µm, while the DVM was 10–50 m, primarily with an ascent at night.

Underlying the apparent size-dependence of MD and DVM for copepods, there was a significant variability in MD and DVM related to stage and taxon. There was a span in MD from 40–50 m for copepodite stages of *Acartia* sp. and *Clausocalanus* sp., to 180–200 m for *Marmonilla* sp. and *Pleuromamma* sp. (Fig. 5b). Between these extremes, the MD's of the other taxa were spread quite evenly. The general range of DVM was 10–20 m, but examples of a wider range of migration were also seen (Fig. 5b and c). Our findings also showed that adults of different species of the same genera can behave quite differently, e.g. *Clausocalanus paulus* vs. *C. furcatus*. and *Oncaea media* vs. *O. mediterranea* (Fig. 5c). This appears, however, not to be in accordance with the general tendency of larger size being at greater depth, given that *Clausocalanus paulus* is smaller than *C. furcatus* (~560 µm vs. ~800 µm) and *Oncaea media* is smaller than. *O. mediterranea* (~370 µm vs. ~660 µm).

Macroplankton

Most of the macroplankton caught by the large ring net were distributed relatively deep at day between 80 and 180 m, and shallower at night above 120 m (Supplementary Table S1). For some taxa within this group, the abundances integrated for the sampled water column were higher during night than during day. Net avoidance at day is unlikely the explanation because these macroplankton cannot visually detect the approaching net; rather, a part of the population may be distributed deeper than our sampling depth at daytime. *Bougainvilla niobe* was among the most numerically abundant; this species migrated from about 130 m at day to 90 m at night (Fig. 4l). The siphonophore *Amphicaryon acaule* showed a strong upward shift in MD from about 160 m to 70 m between day and night (Fig. 4k). Other siphonophores stayed deeper during night–time, and their MD changed from about 150 m at day to 110 m at night (Supplementary Table S1).

Leptocephali larvae

We collected 164 *A. anguilla* and 19 *A. rostrata* larvae during the two series of ring net hauls. The vertical distribution of *A. anguilla* showed a pronounced diel difference:

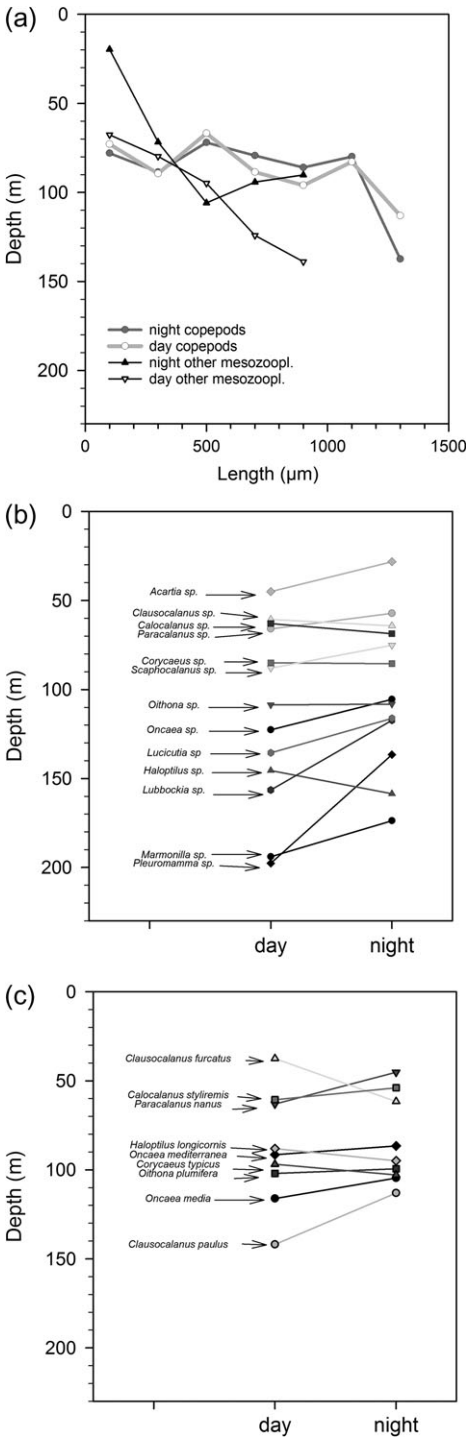

Fig. 5. Day–night changes in depth (m) of the abundant copepod taxa. (**a**) Average length (within intervals of 100 µm) at depth (m) for all copepods. (**b**) Average depth at day versus night for a number of genera in copepodite stages. (**c**) Average depth at day versus night of adult copepods identified to species.

larval abundance peaked at 155 m in daytime (82% of larvae were sampled in the two depth strata 120 m and 155 m), but at night–time larval abundance peaked at 45 m (53% of larvae present at the stratum 45 m; Fig. 6a), and was also more dispersed in the water column. The MD at day was close to the observed depth of peak concentration (160 m vs. 155 m), while at night the MD was somewhat deeper (110 m vs. 45 m) (Fig. 8). Although the diel patterns of vertical distribution of *A. rostrata* were less apparent due to the relatively low catch of this species, findings also indicate peaks in densities at 155 m at day and at 45 m at night (Fig. 6b), while the MDs are slightly shallower than for *A. anguilla* (150 m at day and 90 m at day, Fig. 8). Mean body lengths for *A. anguilla* were 14.1 and 14.5 mm in daytime and night–time samples, respectively, and for *A. rostrata* 14.4 and 17.5 mm, respectively. Larval mean lengths tended to increase with depth at day, whereas no such tendency was seen at night (Fig. 6d and e).

Other species of leptocephali larvae were generally larger than the anguillid leptocephali, and due to visual net avoidance they were poorly represented in the daytime samples. Only the night–time vertical distribution of the combined group of leptocephali larvae is

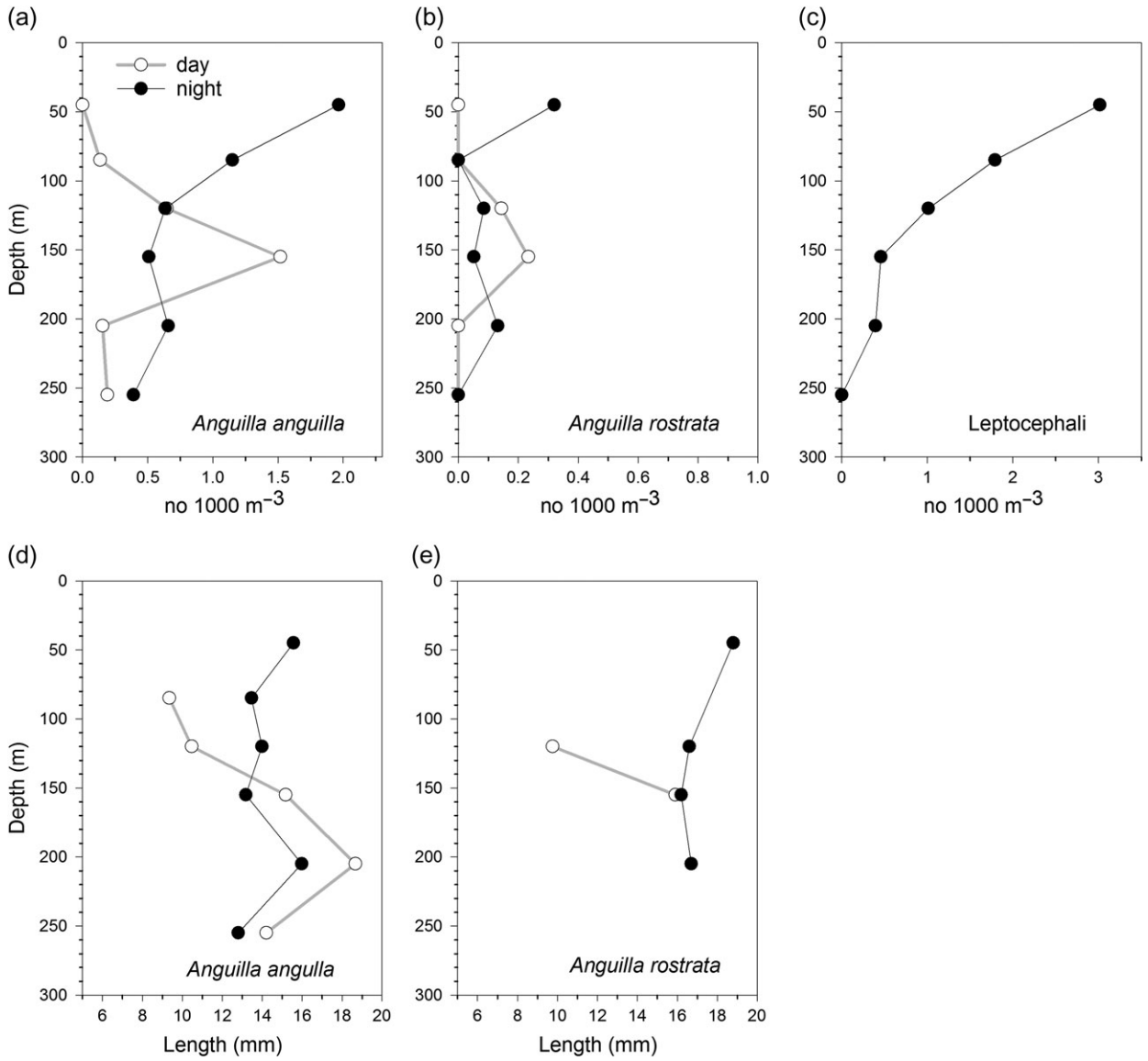

Fig. 6. Vertical distribution and mean sizes of leptocephali species. Day (open symbol) and night (closed symbol) distributions of (**a**) *Anguilla anguilla* and (**b**) *A. rostrata* (no 1000 m^{-3}). (**c**) Night distribution of non-anguillid leptocephali larvae (no 1000 m^{-3}). (**d**) Mean lengths at depth during day and night for (d) *A. anguilla* and (**e**) *A. rostrata* (mm). Based on MIK hauls at nominal depths (symbol ±3 m).

presented here, illustrating the same pattern as for the anguillid larvae: increasing density towards the shallowest stratum of sampling (Fig. 6c).

Other fish larvae

We identified 16 taxonomic groups of fish larvae other than the leptocephali; these were identified to the species or family level (Supplementary Table S1). The diel vertical distribution differed markedly between several of these groups (Fig. 7): Some had their peak distribution at day in the mid-layer (depths 120–155 m) but the concentration could locally be high with almost all larvae found at the same depth (e.g. *Hygphum taaningi*, Fig. 7e), or the larvae could be more dispersed in the lower water column (e.g. *Scopelarchus* sp., Fig. 7b). At night, the overall majority of individuals of each taxon was found at the shallowest depth (e.g. *Evermannellidae* spp., Fig. 7a), in the mid-layer (e.g. *Sternoptychidae diaphana*, Fig. 7f) or at the deepest depth investigated (*Scopelarchus* sp., Fig. 7b). The large variation in distribution patterns of larvae was reflected in their MDs (Fig. 8): two species were either outstandingly shallow (*Ceratoscopelus warmingii*) or deep (*Scopelarchus* sp.), whereas the mean depths of the others were distributed quite evenly between 70 m and 170 m. Both downward and upward migrations between day and night were observed, the vertical migration range was for most species in the order of 20–30 m, but a few species migrated 40–50 m (Fig. 8).

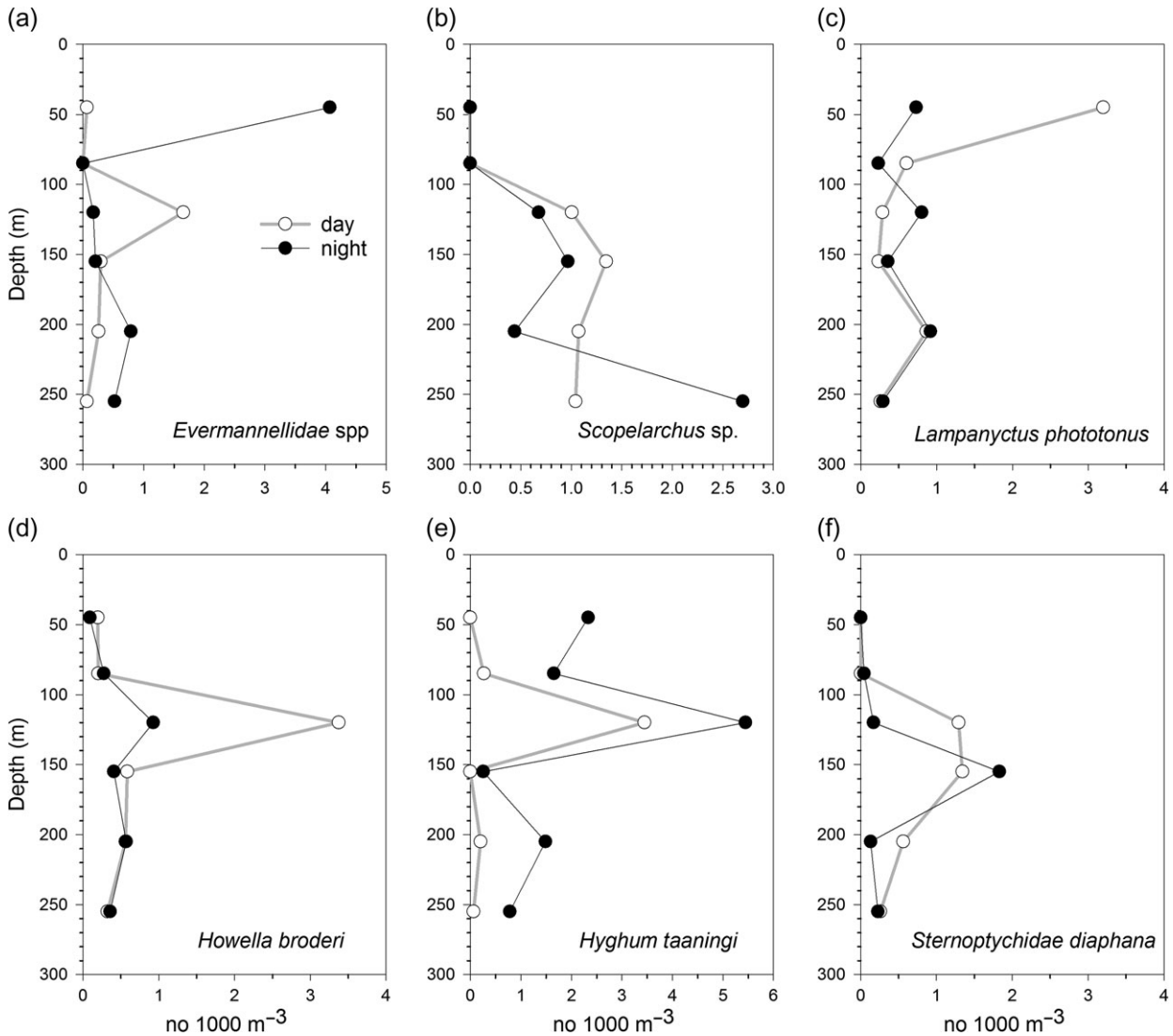

Fig. 7. Vertical distribution of selected fish larvae species based on MIK hauls at nominal depths (symbol ±3 m); values in no. 1000 m^{-3}.

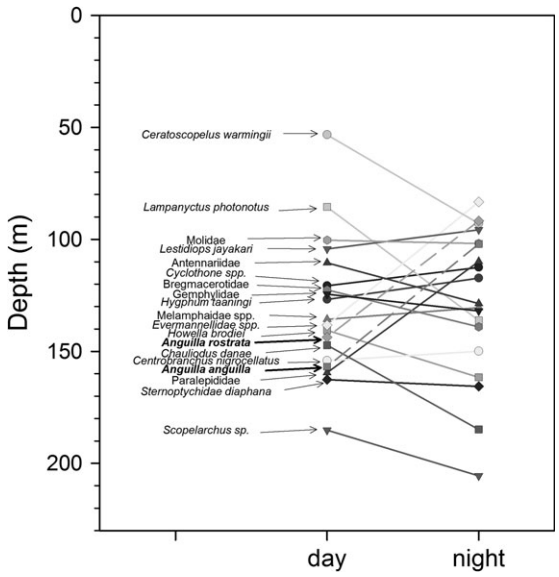

Fig. 8. Average depth (m) at day versus night for common fish larvae species in the area. The two anguillid species are highlighted by bold text and dashed lines.

Fish and other organisms from acoustics

The vertical distribution of organisms reflecting 38 kHz signals was described for a 48-h period, from 1:00 on the 31 March to 23:00 on the 1 April (Fig. 9). At night, acoustic reflections showed an elevated abundance of organisms in the upper 140 m. Separate layers of enhanced reflection were apparent. Just before daybreak (>10 PAR at 10:00 UTM), a group of organisms descended relatively quickly, reaching ~300 m at 10:30 and ~500 m at 12:00. In contrast, other organisms from the series of bands within the upper 250 m showed a more gradual and shorter descent (max. ~50 m descent of separate band), reaching their deepest level at noon when light intensity was at its highest. These migration patterns were reversed after 12:00 UTM, and were repeated in the following 24 h period (Fig. 9).

Plankton community patterns

A cluster analysis on vertical distribution of all abundant mesozooplankton and ichthyoplankton taxa illustrated the diversity of distribution patterns, but also revealed a separation of taxa into distribution types (Supplementary Fig. S1). At a "semi R-square" level above 50% we separated six clusters of distinct characteristics in the daytime sampling (Supplementary Fig. S1a). Three of these showed a characteristic concentration within a single stratum, one of these types, with a concentration in the 85 m stratum, was dominated by mesozooplankton taxa, while fish larvae dominated in two other types (concentration at 45 or 120 m). A large group of taxa was characterized by their bimodal vertical distribution showing peak abundances in the 85 and 155 m strata; this was the general vertical distribution pattern for most of the mesozooplankton. Another group, in which we find the two anguillid eels, constituted a fifth type showing enhanced abundance in the 120 and 155 m strata. The sixth group was found relatively deep (in 155 m stratum or below); however, only few taxa exhibited this distribution pattern. The analysis inferred further clusters within these main clusters, and the general picture of the analysis was a high diversity in patterns of plankton distribution.

DISCUSSION

Our study was focused on plankton distribution in the upper 250 m of the 5000 m deep water column with the expectation that the majority of the community, including the eel larvae, would be distributed here. This interval covers the euphotic zone of sufficient light for primary production and for visual feeding by the fish larvae (about 0.02 μmol m^{-2} s^{-1}; Blaxter, 1980). Further, our observations of a marked decline in abundances of most of the investigated taxa in the deepest sampled stratum (midpoint 255 m) suggest that, by sampling to this depth, we included most of the relevant plankton biomass. The indication in our data that most planktonic organisms in the area had this relatively shallow distribution is supported by findings during studies in other oligotrophic areas which sampled to larger depths (>1000 m). In those studies, modal depths of most investigated plankton species were also found in the interval of 25–150 m (e.g. Longhurst, 1985; Sameoto, 1986). A smaller proportion of the plankton, however, primarily inhabit the deeper layers; e.g. Deevey and Brooks (1977) found in a study off Bermuda that abundances of plankton species residing below 500 m (in the 500–1000 m layer) could be up to 20% of the abundances above 500 m.

The high diversity in plankton distributions in the investigated water layer reflected the large variability in physical conditions. Within the first 250 m of the water column, there was a significant change in light, temperature and water density, and within the pycnocline (80–150 m) we found a strong peak in chlorophyll *a* and a marked intrusion of relatively high-saline water. Thus a wide range of habitual niches are available to the mesozooplankton and ichthyoplankton, and characteristic peaks of distribution within certain depth strata were seen for many organisms. Consequently, the clustering

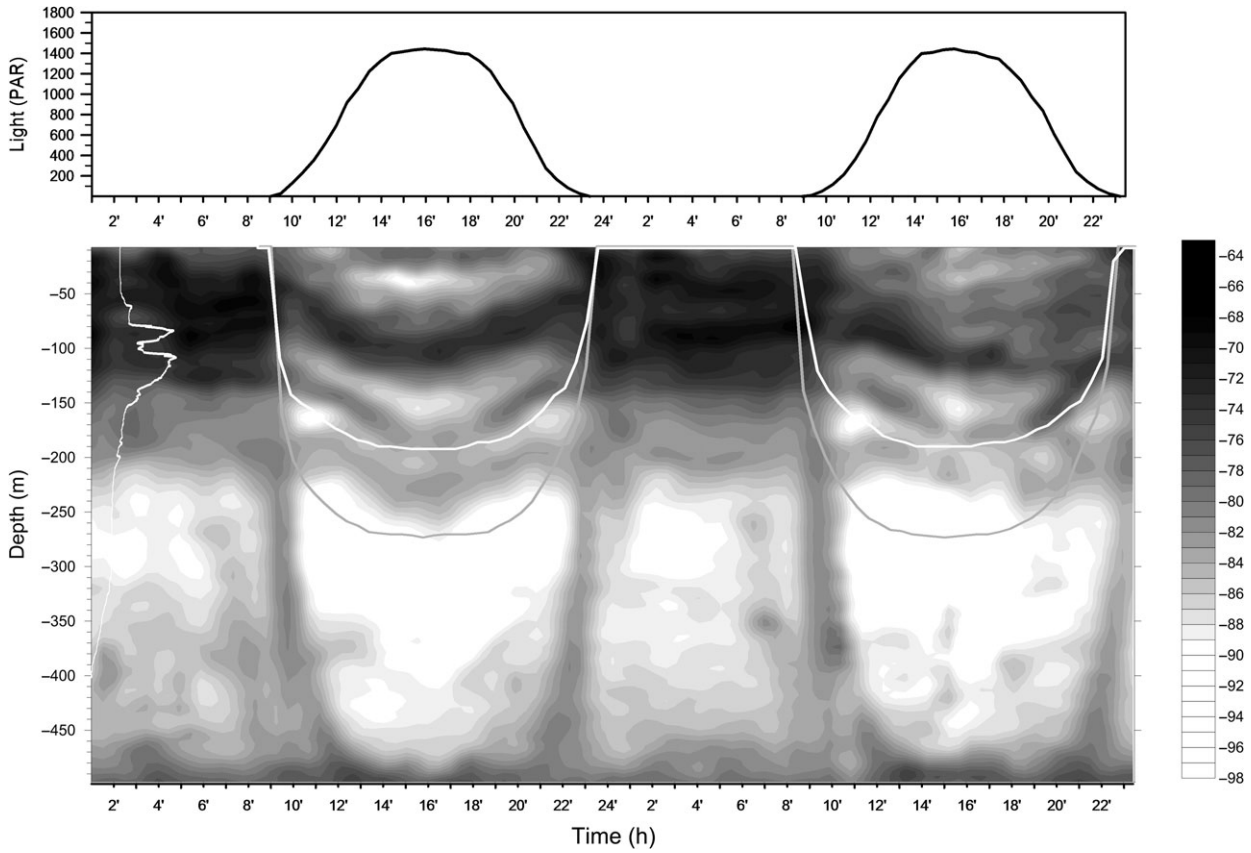

Fig. 9. Lower graph: Acoustic backscatter by ship-mounted 38KHz echo sounder, in dB, as given by bar to the right. From 01:00 (UTM) on the 31 March to 23:00 on the 1 April. White line off left axis illustrates the salinity profile; lines undulating to depth illustrate calculated depths of given light intensities; white upper line: 1.5 μmol m^{-2} s^{-1}, gray lower line: 0.02 μmol m^{-2} s^{-1}. Upper graph: surface light intensity during the same period, from ship-mounted PAR sensor.

of organisms based on distributional similarities showed that in addition to bulk-water characteristics, there were also significant fine-scale variabilities that influenced the distributional patterns for both mesozooplankton and ichthyoplankton.

A large number of the investigated taxa showed systematic polymodality in their vertical distribution. The layer immediately below the uppermost surface (measured at 45 m depth) appeared unsuitable for most taxa, leading to low abundances here. While the mesozooplankton organisms often were abundant above (12 m stratum) and below (85 m stratum); this led to two modes in the vertical distribution. For many organisms there was a tendency of another low in abundance at the central pycnocline at about 120 m, within the salinity intrusion and the chlorophyll *a* maximum. This tendency of several modes in distribution was seen for much of the mesozooplankton, both during daytime and night–time sampling, while for the ichthyoplankton the pattern of distribution was unimodal for most taxa.

The concentration at specific depth was evident for the two anguillid eel larvae. At daytime, the larvae congregated in the 155 m stratum at a concentration about seven times as high as the average of the other abundance estimates in the water column, and at night–time the concentration in the 45 m stratum was three times as high as the average of other estimates. Thus, at the investigated site, most of the anguillid leptocephali were below 100 m at daytime while the majority migrated to above 100 m depth at night. Interestingly, peaks in eel larvae distribution coincided with peaks in abundances of sampled hydrozoans, as apparent when comparing Fig. 6a and b with Fig. 5k and l. The hydrozoans have been proposed as possible food items for the leptocephali larvae (Riemann *et al.* 2010), and a study from the same cruise found eel larval gut contents dominated by gene sequences of taxa belonging to Hydrozoa (Ayala *et al.*, 2018).

The observations of a deeper distribution of anguillid eel larvae during daytime, and a shallower distribution during night–time are in accordance with other findings

for the species during the winter/spring period. Castonguay and McCleave (1987) found significant abundance peaks in specific depth strata as well: In their study, the maximal concentration at depth was seen at night and was here about nine times the average of the other depth strata. Accordingly, the day and night peak concentrations of larvae occurred within the wide pycnocline, and the tendency of an increase in larval mean length with increasing sampling depth during daytime are also apparent in the data presented by Schoth and Tesch (1984).

The observed diel migration (~70 m) of *Anguilla* sp. was of exceptional magnitude compared to migrations of most other fish larvae in our study, which ranged only 10–30 m. Migration distances of oceanic fish larvae are commonly in the lower range; for example, in a study of the fish larval community off the Canary Islands, Rodríguez *et al.* (2006) observed relatively short migration distances of 5–20 m for most species, and similar to our study, they observed both upward and downward migrations during night. The different species of fish larvae we observed apparently utilized different parts of the water column; some were concentrated in relatively deep water, some in the shallow layer, and others were more dispersed in the mid-layer. Thus, while the vertical distributions of fish larvae overlapped to different degrees, the calculated midpoints of distributions extended throughout much of the water column.

We used acoustic measurements and the diel movement of bands of enhanced backscatter to describe migratory patterns of plankton and fish at a finer temporal scale than our day–night sampling. Stratification of the backscatter is a common observation in acoustic surveys, and the different bands of enhanced backscatter have been related to different taxonomic composition of organisms (e.g. Lawson *et al.*, 2004). While we cannot directly link certain bands to specific taxa, the patterns of backscatter in the uppermost water column during night are in accordance with the observations of peaking distributions of organisms in the pycnocline and around the high-saline intrusion at 80–130 m depth (Fig. 9).

The acoustic observations complement our day–night sampling by showing the diel migration as a gradual descent to, and ascent from, the deepest positions of given organisms. The descent was initiated at the first light at the surface, and the return was finished at time of complete darkness. Successively, the vertical positions of organisms were stable during night, with a slight tendency of deeper distribution at midnight, until a new descent in the morning. From the acoustic measurements, the general migration distances in the upper part of the water column were interpreted to be about 50 m, which is in the upper range compared to migration distances of most of the (smaller) organisms that were included in our day–night sampling campaign. The descent of the upper set of distribution bands reached to ~270 m, which is within the range of the general light threshold for larval fish feeding (Fig. 9). In the echogram, some bands of acoustic backscatter apparent at night descended much deeper than the 50 m; these are likely related to movement of mesopelagic fish which are commonly observed to descend to more than 500 m depth (e.g. Badcock and Merrett, 1976; D'Elia *et al.*, 2016).

In conclusion, the study illustrates the great physical and biological variabilities of the area of eel larvae distribution at STCZ, and points out a range of commonalities and differences between plankton taxa at the mesozooplankton and ichthyoplankton levels. Irrespective of the oligotrophic nature of this oceanic area, the diversity of the plankton community—in terms of taxonomy and distribution patters—was notably high. Plankton organisms were highly concentrated in specific strata, and several peaks in their vertical distribution could often be seen. These presumably are linked to the variable hydrography around the pycnocline. The anguillid eels concentrate in the lower part of the pycnocline at daytime, and their prevalence in a water layer with enhanced abundances of hydrozoans indicates these organisms as potential prey item for the eel larvae. For further understanding and modeling of the early life characteristics of eel across their extensive area of distribution, it is necessary to incorporate the prominent small-scale variability and diversity of their immediate physical and biological environments.

SUPPLEMENTARY DATA

Supplementary data can be found online at *Journal of Plankton Research online.*

ACKNOWLEDGEMENTS

We thank colleagues and the crew of the Danish research vessel, DANA, for their helpful assistance during field sampling and sample processing.

FUNDING

This study was supported by the Carlsberg Foundation, Denmark (2012_01_0272); Danish Centre for Marine Research (2013_02) and the Danish Council for

Independent Research/Marie Curie (Mobilex: DFF-1325-00102B to CJ).

REFERENCES

Andersen, N. G., Nielsen, T. G., Jakobsen, H. H., Munk, P. and Riemann, L. (2011) Distribution and production of plankton communities in the subtropical convergence zone of the Sargasso Sea. II. Protozooplankton and copepods. *Mar. Ecol. Prog. Ser.*, **426**, 71–86.

Ayala, D. J., Munk, P., Lundgreen, R. B. C., Traving, S. J., Jaspers, C., Jørgensen, T. S., Hansen, L. H. and Riemann, L. (2018) Gelatinous plankton is central to the diet of European eel (Anguilla anguilla) larvae in the Sargasso Sea. Scientific Reports, **8**, 6156.

Ayala, D., Riemann, L. and Munk, P. (2016) Species composition and diversity of fish larvae in the subtropical convergence zone of the Sargasso Sea from morphology and DNA barcoding. *Fish. Oceanogr.*, **25**, 85–104.

Badcock, J. and Merrett, N. R. (1976) Midwater fishes in the eastern North Atlantic—I. Vertical distribution and associated biology in 30 N, 23 W, with developmental notes on certain myctophids. *Prog. Oceanogr.*, **7**, 3–58.

Blaxter, J. H. S. (1980) Vision and feeding of fishes. In *Fish Behaviour and its Use in the Capture and Culture of Fishes*, Vol. 5. International Center for Living Aquatic Resources Management, Manila, Philippines, pp. 32–56.

Bouillon, J., Medel, M. D., Pages, F., Gili, J. M., Boero, F. and Gravili, C. (2004) Fauna of the Mediterranean hydrozoa. *Sci. Mar.*, **68**, 5–449.

Castonguay, M. and McCleave, J. D. (1987) Vertical distributions, diel and ontogenetic vertical migrations and net avoidance of leptocephali of Anguilla and other common species in the Sargasso Sea. *J. Plankton Res.*, **9**, 195–214.

Cushman-Roisin, B. (1984) On the maintenance of the subtropical front and its associated countercurrent. *J. Phys. Oceanogr.*, **14**, 1179–1190.

Deevey, G. B. and Brooks, A. L. (1977) Copepods of the Sargasso Sea off Bermuda: species composition, and vertical and seasonal distribution between the surface and 2000 m. *Bull. Mar. Sci.*, **27**, 256–291.

D'elia, M., Warren, J. D., Rodriguez-Pinto, I., Sutton, T. T., Cook, A. and Boswell, K. M. (2016) Diel variation in the vertical distribution of deep-water scattering layers in the Gulf of Mexico. *Deep Sea Res. I*, **115**, 91–102 http://dx.doi.org/10.1016/j.dsr.2016.05.014.

Eriksen, C. C., Weller, R. A., Rudnick, D. L., Pollard, R. T. and Regier, L. A. (1991) Ocean frontal variability in the frontal air-sea interaction experiment. *J. Geophys. Res.*, **96**, 8569–8591.

Gasol, J. M., del Giorgio, P. A. and Duarte, C. M. (1997) Biomass distribution in marine planktonic communities. *Limnol. Oceanogr.*, **42**, 1353–1363.

Halliwell, G. R., Jr, Ro, Y. J. and Cornillon, P. (1991) Westward-propagating SST anomalies and baroclinic eddies in the Sargasso Sea. *J. Phys. Oceanogr.*, **21**, 1664–1680.

Jacobsen, M. W., Smedegaard, L., Sørensen, S. R., Pujolar, J. M., Munk, P., Jónsson, B., Magnussen, E. and Hansen, M. M. (2017) Assessing pre-and post-zygotic barriers between North Atlantic eels (*Anguilla anguilla* and *A. rostrata*). *Heredity*, **118**, 266.

Lawson, G. L., Peter, H. W., Ashjian, C. J., Gallager, S. M., Davis, C. S. and Warren, J. D. (2004) Acoustically-inferred zooplankton distribution in relation to hydrography west of the Antarctic Peninsula. *Deep Sea Res. II*, **51**, 2041–2072.

Longhurst, A. R. (1985) The structure and evolution of plankton communities. *Prog. Oceanogr.*, **15**, 1–35.

Miller, M. J. (2015) Nighttime vertical distribution and regional species composition of eel larvae in the western Sargasso Sea. *Reg. Stud. Mar. Sci.*, **1**, 34–46.

Miller, M. J., Bonhommeau, S., Munk, P., Castonguay, M., Hanel, R. and McCleave, J. D. (2014) A century of research on the larval distributions of the Atlantic eels: a re-examination of the data. *CCCC Rev.*, **90**, 1035–1064.

Munk, P., Hansen, M. M., Maes, G. E., Nielsen, T. G., Castonguay, M., Riemann, L. and Bachler, M. (2010) Oceanic fronts in the Sargasso Sea control the early life and drift of Atlantic eels. *Proc. R. Soc. of Lond. B Biol. Sci.*, **277**, 3593–3599.

Richardson, K. and Bendtsen, J. (2017) Photosynthetic oxygen production in a warmer ocean: the Sargasso Sea as a case study. *Phil. Trans. R. Soc. A*, **375**, 20160329.

Riemann, L., Alfredsson, H., Hansen, M. M., *et al.* (2010) Qualitative assessment of the diet of European eel larvae in the Sargasso Sea resolved by DNA barcoding. *Biol. Lett.*, **6**, 819–822.

Riemann, L., Nielsen, T. G., Kragh, T., Richardson, K., Parner, H., Jakobsen, H. H. and Munk, P. (2011) Distribution and production of plankton communities in the subtropical convergence zone of the Sargasso Sea. I. Phytoplankton and bacterioplankton. *Mar. Ecol. Prog. Ser.*, **426**, 57–70.

Rodríguez, J. M., Hernández-León, S. and Barton, E. D. (2006) Vertical distribution of fish larvae in the Canaries-African coastal transition zone in summer. *Mar. Biol.*, **149**, 885–897.

Sameoto, D. D. (1986) Influence of the biological and physical environment on the vertical distribution of mesozooplankton and micronekton in the eastern tropical Pacific. *Mar. Biol.*, **93**, 263–279.

Schmidt, J. (1923) The breed places of the eel. *Philos. Trans. R. Soc. Lond. B*, **211**, 179–208.

Schoth, M. and Tesch, F. W. (1982) Spatial distribution of 0-group eel larvae (*Anguilla* sp.) in the Sargasso Sea. *Helgoländer Meeresuntersuchungen*, **35**, 309.

Schoth, M. and Tesch, F. W. (1984) The vertical distribution of small 0-group *Anguilla* larvae in the Sargasso Sea with reference to other anguilliform leptocephali. *Kieler Meeresforsch.*, **30**, 188–195.

Steinberg, D. K., Carlson, C. A., Bates, N. R., Johnson, R. J., Michaels, A. F. and Knap, A. H. (2001) Overview of the US JGOFS Bermuda Atlantic Time-series Study (BATS): a decade-scale look at ocean biology and biogeochemistry. *Deep Sea Res. II*, **48**, 1405–1447.

Ullman, D. S., Cornillon, P. C. and Shan, Z. (2007) On the characteristics of subtropical fronts in the North Atlantic. *J. Geophys. Res.*, **112**, C01010.

Williams, R. G. (2001) Ocean subduction. In Steele, J. H., Turekian, K. K. and Thorpe, S. A. (eds), *Encyclopedia of Ocean Sciences*. San Diego, CA: Academic Press, pp. 1982–1992.